Theory of Underdoped Cuprates

Xiao-Gang Wen and Patrick A. Lee

Department of Physics, Massachusetts Institute of Technology, Cambridge, Massachusetts 02139
(Received 15 June 1995)

We develop a slave-boson theory for the *t-J* model at finite doping which respects an SU(2) symmetry—a symmetry previously known to be important at half filling. The mean field phase diagram is found to be consistent with the phases observed in the cuprate superconductors, which contain *d*-wave superconductor, spin gap, strange metal, and Fermi liquid phases. The spin gap phase is best understood as the staggered flux phase, which is nevertheless translationally invariant for physical quantities. The electron spectral function shows small Fermi pockets at low doping which continuously evolve into the large Fermi surface at high doping concentrations.

The parent compound of the cuprate superconductors is an antiferromagnetic (AF) insulator. With hole doping, AF is rapidly destroyed and a metallic state emerges. It is well established that at optimal doping a Fermi surface exists with area $1 - x$, where x is the concentration of doped holes [1]. On the other hand, for $x \ll 1$, the system remains AF with a doubled unit cell, and the Fermi surface is expected to be small pockets centered around the $(\pi/2, \pi/2)$ point [2]. An important question is how the low lying electron state evolves from small x to optimal doping. This intermediate region, called the underdoped regime, also exhibits unusual magnetic properties often referred to as spin gap behavior. Unlike optimally doped systems, where the magnetic susceptibility χ is temperature independent, underdoped cuprates generally show a reduction in χ at temperatures below 400 K or so [3]. Below 150 K, χ and the NMR relaxation rate decrease abruptly in an activated manner. It has been argued that this is observed only in bilayer materials [3]. In this paper we shall concentrate only on the high temperature spin gap behavior, which we view as evidence for the formation of spin singlets within the Cu-O layer. We shall address the question of how the spin gap manifests itself in the electronic spectral function, and how the Fermi surface evolves from small pockets to a large Fermi surface which satisfies Luttinger's theorem. This last question was addressed in a weak coupling theory [4], where fluctuating spin density waves induce shadow bands. We would like to study the strong correlation limit which we believe to be more appropriate for the cuprates, and we take the *t-J* model as our starting point.

A standard way of enforcing the constraint of no double occupancy of the *t-J* model is to write the electron operator $c_{\alpha i}$ in terms of auxiliary fermions and boson particles $c_{\alpha i} = f_{\alpha i} b_i^\dagger$ and demand that each site is occupied by either a fermion or a boson. In a mean field (MF) treatment, the order parameters $\chi_{ij} = \langle f_{\alpha i}^\dagger f_{\alpha j} \rangle$ and $\Delta_{ij} = \langle f_{1i} f_{2j} - f_{2i} f_{1j} \rangle$ describe the formation of singlets envisioned in Anderson's resonating valence bond (RVB) picture [5]. At zero doping, the translationally

invariant solution can be described as a π-flux phase [6] or a d-wave pairing state with $|\Delta_{ij}| = |\chi_{ij}|$. The symmetry which underlies the degenerate MF states has been identified as SU(2), which expresses the idea that a physical up spin can be viewed as either the presence of an up spin or the absence of a down spin fermion [7]. In the conventional theory, the SU(2) is broken to U(1) upon doping, and only the d-wave state survives as the MF solution [8,9]. This scenario has been used as an explanation of the spin gap phenomenon [9].

In this paper we present a new formulation of the constraint which preserves SU(2) symmetry away from half filling. Our hope is that, since SU(2) is an exact symmetry at half filling, the MF approximation of the new formulation may capture more accurately the low energy degrees of freedom and may be a better starting point for small x. We are also motivated by the photoemission experiment on the insulating cuprate [10], which finds a large excitation energy at the $(0, \pi)$ point, comparable to that at $(0, 0)$. This is just what is expected from the π-flux phase spectrum, suggesting that the AF state may resemble the π-flux phase at short distances. As we shall see, the SU(2) formulation provides a scenario for how the π-flux phase is connected to the spin gap phase and how the hole pockets evolve upon doping.

The SU(2) doublets $\psi_{1i} = \begin{pmatrix} f_{1i} \\ f_{2i}^\dagger \end{pmatrix}$ and $\psi_{2i} = \begin{pmatrix} f_{2i} \\ -f_{1i}^\dagger \end{pmatrix}$ were introduced in Ref. [7]. Here we introduce *two* spin-0 boson fields b_a, $a = 1, 2$, forming another doublet $b_i = \begin{pmatrix} b_{1i} \\ b_{2i} \end{pmatrix}$. We then form SU(2) singlets to represent the physical operators $\vec{S}_i = \frac{1}{2} f_{\alpha i}^\dagger \vec{\sigma}_{\alpha\beta} f_{\beta i}$, $c_{1i} = b_i^\dagger \psi_{1i}/\sqrt{2} = (b_{1i}^\dagger f_{1i} + b_{2i}^\dagger f_{2i}^\dagger)/\sqrt{2}$, and $c_{2i} = b_i^\dagger \psi_{2i}/\sqrt{2} = (b_{1i}^\dagger f_{2i} - b_{2i}^\dagger f_{1i}^\dagger)/\sqrt{2}$. The *t-J* Hamiltonian $\sum_{(ij)} [J(\vec{S}_i \cdot \vec{S}_j - \frac{1}{4} n_i n_j) - t(c_{\alpha i}^\dagger c_{\alpha j} + \text{H.c.})]$ can now be written in terms of our fermion-boson (FB) fields. The Hilbert space of the FB system is larger than that of the *t-J* model. However, the local SU(2) singlets satisfying $(\frac{1}{2} \psi_{\alpha i}^\dagger \vec{\tau} \psi_{\alpha i} + b_i^\dagger \vec{\tau} b_i)|\text{phys}\rangle = 0$ form a subspace that is identical to the Hilbert space of the *t-J* model. On a given site, there are only three states that

satisfy the above constraint. They are $f_1^\dagger|0\rangle$, $f_2^\dagger|0\rangle$, and $\frac{1}{\sqrt{2}}(b_1^\dagger + b_2^\dagger f_2^\dagger f_1^\dagger)|0\rangle$, corresponding to a spin up and down electron, and a vacancy, respectively. Furthermore, the FB Hamiltonian, as an SU(2) singlet operator, acts within the subspace, and has the same matrix elements as the t-J Hamiltonian.

Following the standard approach, we obtain the following MF Hamiltonian [11] for the FB system:

$$H_m = -\mu \sum_i b_i^\dagger b_i - \sum_i a_{0i}^l \left(\frac{1}{2}\psi_{\alpha i}^\dagger \tau^l \psi_{\alpha i} + b_i^\dagger \tau^l b_i\right)$$
$$+ \sum_{(i,j)} \frac{3J}{8}(|\chi_{ij}|^2 + |\Delta_{ij}|^2 + \psi_{\alpha i}^\dagger U_{ij}\psi_{\alpha j})$$
$$+ t(b_i^\dagger U_{ij} b_j + \text{H.c.}), \qquad (1)$$

where $U_{ij} = \begin{pmatrix} -\chi_{ij}^* & \Delta_{ij} \\ \Delta_{ij}^* & \chi_{ij} \end{pmatrix}$.

The first two terms of H_m are included to impose the constraints. The value of μ is chosen such that the total boson density (which is also the density of the holes in the t-J model) is $\langle b_i^\dagger b_i\rangle = \langle b_{1i}^\dagger b_{1i} + b_{2i}^\dagger b_{2i}\rangle = x$. The values of a_{0i}^l are chosen such that $\langle \frac{1}{2}\psi_{\alpha i}^\dagger \tau^l \psi_{\alpha i} + b_i^\dagger \tau^l b_i\rangle = 0$. For $l = 3$ we have

$$\langle f_{\alpha i}^\dagger f_{\alpha i} + b_{1i}^\dagger b_{1i} - b_{2i}^\dagger b_{2i}\rangle = 1. \qquad (2)$$

We see that, unlike the U(1) case, the density of the fermions $\langle f_{\alpha i}^\dagger f_{\alpha i}\rangle$ is not necessarily equal to $1 - x$. This is because a vacancy in the t-J model may be represented by an empty site with a b_1 boson or a doubly occupied site with a b_2 boson. We also notice that the MF Hamiltonian is invariant under local SU(2) transformations, $W_i \in$ SU(2): $\psi_{\alpha i} \to W_i \psi_{\alpha i}$, $b_i \to W_i b_i$, $U_{ij} \to W_i U_{ij} W_j^\dagger$, and $a_{0i}^l \tau^l \to W_i a_{0i}^l \tau^l W_i^\dagger$.

We have searched the minima of the MF free energy for the MF ansatz with translation, lattice, and spin rotation symmetries. We find a phase diagram with six different phases (Fig. 1).
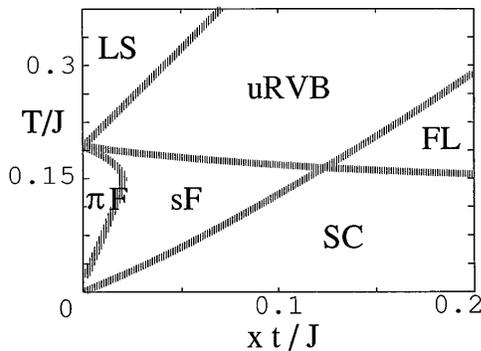
FIG. 1. SU(2) MF phase diagram for $t/J = 1$. The phase diagram for $t/J = 2$ is quantitatively very similar to the $t/J = 1$ phase diagram, when plotted in terms of the scaled variable xt/J, except the πF phase disappears at a lower scaled doping concentration.

(1) Staggered flux (sF) phase:

$$U_{i,i+\hat{x}} = -\tau^3 \chi - i(-)^{i_x+i_y}\Delta,$$
$$U_{i,i+\hat{y}} = -\tau^3 \chi + i(-)^{i_x+i_y}\Delta, \qquad (3)$$

and $a_{0i}^l = 0$. In the U(1) slave-boson theory, the staggered flux phase breaks translation symmetry. Here the breaking of translational invariance is a gauge artifact. In fact, a site dependent SU(2) transformation $W_i = \exp[i(-1)^{i_x+i_y}(\pi/4)\tau_1]$ maps the sF phase to the d-wave pairing phase of the fermions: $U_{i,i+\hat{x},\hat{y}} = -\chi\tau_3 \pm \Delta\tau_1$, which is explicitly translationally invariant. In the sF phase the fermion and boson dispersions are given by $\pm E_f$ and $\pm E_b$, where $E_f = \sqrt{(\epsilon_f - a_0^3)^2 + \eta_f^2}$, $\epsilon_f = -(3J/4)(\cos k_x + \cos k_y)\chi$, $\eta_f = -(3J/4)(\cos k_x - \cos k_y)\Delta$, and a similar result for E_b with $3J/4$ replaced by $2t$. Since $a_0^3 = 0$, we have $\langle f_{\alpha i}^\dagger f_{\alpha i}\rangle = 1$ and $\langle b_1^\dagger b_1\rangle = \langle b_2^\dagger b_2\rangle = x/2$.

(2) The π-flux (πF) phase is the same as the sF phase except here $\chi = \Delta$.

(3) The uniform RVB (uRVB) phase is described by Eq. (3) with $a_{0i}^l = \Delta = 0$.

(4) A localized spin (LS) phase has $U_{ij} = 0$ and $a_{0i}^l = 0$, where the fermions cannot hop.

(5) The d-wave superconducting (SC) phase is described by $U_{i,i+\hat{x},\hat{y}} = -\chi\tau_3 \pm \Delta\tau_1$ and $a_0^3 \neq 0$, $a_0^{1,2} = 0$, $\langle b_1\rangle \neq 0$, $\langle b_2\rangle = 0$. Notice that the boson condenses in the SC phase despite the fact that in our MF theory the interactions between the bosons are ignored. The SC MF solution provides an interesting example of finite-temperature free boson condensation in two dimensions. To see this, notice that the a_0^3 term in the FB Hamiltonian $-\sum_i a_0^3(f_{\alpha i}^\dagger f_{\alpha i} + b_{1i}^\dagger b_{1i} - b_{2i}^\dagger b_{2i} - 1)$ makes a_0^3 behave like the chemical potential of the fermions. The fermions favor a nonzero a_0^3. Let us assume $a_0^3 < 0$, which makes $\langle f_{\alpha i}^\dagger f_{\alpha i}\rangle < 1$. A negative a_0^3 also makes the b_1-band bottom higher than that of b_2, and the thermally excited bosons satisfy $\langle b_1^\dagger b_1\rangle_{\text{therm}} < \langle b_2^\dagger b_2\rangle_{\text{therm}}$. Thus the thermally excited bosons alone cannot satisfy the constraint in Eq. (2). The b_1 bosons are forced to condense at the bottom of the b_1 band to satisfy the constraint, in the same way that ordinary bosons condense to satisfy the density constraint. Because of the fermion contribution, the total free energy can still be lowered by generating a finite a_0^3 at low temperatures.

(6) The Fermi liquid (FL) phase is similar to the SC phase except that there is no fermion pairing ($\Delta = 0$).

In the following we would like to discuss some simple physical properties of the MF phases. uRVB, sF, πF, and LS phases contain no boson condensation and correspond to unusual metallic states. Since $a_0^3 = 0$, the area of the fermion Fermi sea in the uRVB phase is pinned at $\frac{1}{2}$ of the Brillouin zone. As the temperature is

lowered, fermions condense in pairs or develop staggered flux and the uRVB phase changes into the sF or πF phase. A gap is opened at the Fermi surface which reduces the low energy spin excitations. Thus the sF and πF phases correspond to the high temperature spin gap phase. The SC phase contains both the boson and fermion pair condensations and corresponds to a d-wave superconducting state of the electrons. The FL phase containing boson condensation corresponds to a Fermi liquid phase of electrons. However, the area of the Fermi sea produced by the SU(2) MF theory is larger than that predicted by the Luttinger theorem, which reveals a drawback of the SU(2) MF theory at high doping concentrations. This is probably related to another drawback of the SU(2) theory that the superconducting T_c goes down too slowly beyond the optimal doping. It appears that the U(1) MF theory is better at higher doping.

We would like to point out that the different MF phases contain different gauge symmetries. The uRVB and the πF phases have the full SU(2) gauge symmetry. In the sF phase the SU(2) gauge symmetry is broken down to U(1) [12], while in the SC and FL phases the SU(2) gauge symmetry is completely broken.

Next we calculate the physical electron Green function in the sF phase. Using the expression of c_α, the MF approximation G_0 is given by the convolution of fermion and boson Green functions. The expression of G_0 is lengthy, but can be approximated at low temperatures by

$$G_0(k, \omega) = \frac{x}{2}\left(\frac{u^2}{\omega - E_f} + \frac{v^2}{\omega + E_f}\right) + G_{in}. \quad (4)$$

The first term describes the coherent motion of electrons with the fermion dispersion (where a finite decay rate of order T is ignored). The new feature is the appearance of the coherent factors $u(k) = \sqrt{(E_f + \epsilon_f)/2E_f} \, \text{sgn}(\eta_f)$ and $v(k) = \sqrt{(E_f - \epsilon_f)/2E_f}$. The second term is the incoherent background, which mainly reflects the boson density of states. $\text{Im}G_{in}$ exists only for $\omega < 0$ and contributes $1/2$ to a total spectral weight $(1 + x)/2$.

The coherent part of G_0 produces only Fermi points at $\Sigma = (\pm\pi/2, \pm\pi/2)$. Another feature is that the occupied part of the spectral weight of G_0 contains $1 + x/2$ electrons as opposed to $1 - x$ electrons. These unsatisfactory features are due to the absence of correlation between fermions and bosons in arriving at G_0. In reality there is a strong attraction between them due to gauge fluctuations. In the limit of a single hole, this attraction can lead to a bound state with the quantum number of an electron, as emphasized in Ref. [13]. In the case of finite hole concentration, we expect that fermion particle-hole pairs may be spontaneously excited out of the MF ground state so that the b_2 (b_1) bosons can bind to fermions (antifermions). The result would be low lying physical electron excitations which may resemble a Fermi surface. In order to capture this physics, even at a very crude level,

we assume that after screening the a_0^l fluctuations induce the short range interaction $-\sum_i U\psi_{\alpha i}^\dagger \tau^l \psi_{\alpha i} b_i^\dagger \tau^l b_i$, where $U < 0$. We have calculated G_U, which includes this attraction, in the Bethe-Salpeter approximation. The results are shown in Figs. 2 and 3. To interpret these results, we consider instead $G_U' = (G_0^{-1} + U)^{-1}$, which we have found numerically to be nearly identical to G_U. It is easy to see that G_U' also has the form $G_U' = G_{coh}' + G_{in}'$. In the case when either $|u|$ or $|v| \approx 1$, we find that $G_{coh}' = Z/(\omega \pm E_f + \mu_f)$ with $\mu_f = xU/2(1 + UG_{in})$ and $Z = (x/2)/(1 + UG_{in})^2$. We see that a negative U generates a negative μ_f which produces small hole pockets. A negative U also enhances the spectral weight of unoccupied quasiparticles. This allows us to choose U by requiring that the occupied spectral weight in G_U is $1 - x$. For general u and v, we find that the coherent part of G_U' produces pocketlike Fermi surfaces near Σ (see Fig. 2), which are determined by $2E_f(1 + UG_{in}) = Ux(u^2 - v^2)$. The quasiparticle weight at the Fermi surface $Z = 2E_f^2/xU^2$ vanishes at Σ and is very small on the outer edge of the pocket, making it hard to detect. As we approach the uRVB phase, Δ decreases and the pockets are elongated, while their area increases with doping. Eventually the inner edges of the pockets join together to form a large Fermi surface, with low lying excitations near M and a shape which resembles the experiment [1].

The incoherent background of $\text{Im}G_U$ contains two broad peaks separated by $2t$, shown in Fig. 2(a) at Σ and M. This follows from the pseudogap in the boson density of states and is a direct consequence of the staggered flux. Coherence factors cause a transfer of spectral weight from the low energy to the high energy peak as one goes from Γ to Σ to X [14], in qualitative agreement with exact diagonalization results [15] with the same doping concentration but at a higher temperature.
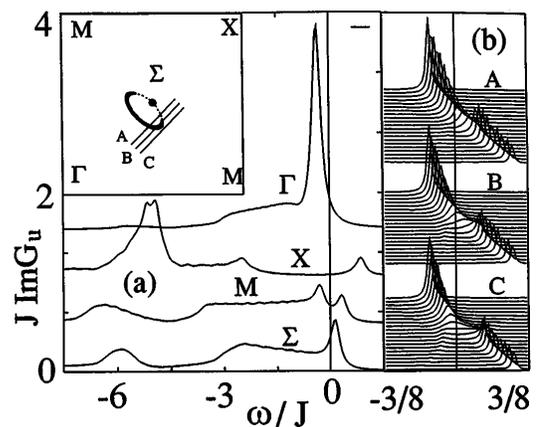
FIG. 2. (a) The electron spectral function $\text{Im}G_U$ in the sF phase for $t/J = 2$, $x = 0.041$, and $T/J = 0.13$, where $\chi = 0.57$ and $\Delta = 0.22$. The sharp peaks near $\omega = 0$ are quasiparticle peaks. The inset shows a quarter of the Brillouin zone. (b) The spectral functions $\text{Im}G_U$ for three linear scans along the lines A, B, and C in the inset.
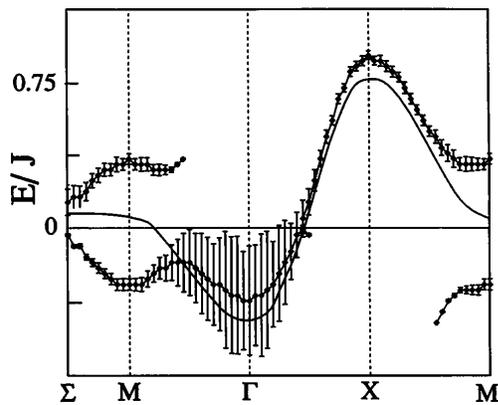
FIG. 3. The points describe the dispersion of the quasiparticle peaks for the sF phase in Fig. 2. The vertical bars are proportional to the peak values of ImG_U, which reflect the quasiparticle weight. The solid curve is the quasiparticle dispersion for a uRVB phase with the same doping concentration but at a higher temperature ($T/J = 0.19$).

Figure 3 shows the dispersion of the quasiparticle peaks and their spectral weights. Comparing the sF and uRVB dispersions, we see clearly a splitting of the spectral weight along Σ to M, which is remarkable for a translational invariant state. In our theory the splitting is naturally related to the spin gap. We also note that at half filling the bottoms of the band at M and Γ are degenerate. As doping is increased, the spin gap shrinks and the occupied band near M moves up in energy, eventually producing the flat band near the Fermi surface seen in photoemission experiments. In our calculation, the band at Γ has been pushed up in energy from its bare value near $-J$ to $-J/2$ due to the inclusion of U, whereas the experimental value is closer to $-2J$. We believe this feature, as well as the large spectral weight near Γ, is an artifact of our crude treatment of the gauge fluctuation.

Figure 2(b) shows, in more detail, how the Fermi surface disappears in the sF phase. In scan C, a ghost band below the Fermi energy is quite visible after the main peak goes above the Fermi surface. This band is connected to the occupied band in Fig. 3 as the M point is approached. The appearance of the ghost band and the sudden reduction of the quasiparticle spectral weight in the ghost band have been observed in the insulating cuprates [10]. The inner edge of the Fermi pocket in the inset of Fig. 2 is determined from the position of the quasiparticle peaks at $\omega = 0$. The quasiparticle peaks at the outer edge of the Fermi pocket are not visible in our numerical result, and the full ellipse of the Fermi pocket is completed based on our analytic results on G'_U.

The SU(2) MF theory shares many similar physical properties with the U(1) MF theory (where the spin gap is generated by the d-wave pairing of the fermions). However, there are some qualitative distinctions. (1)

The sF phase in the SU(2) theory contains a gapless U(1) gauge field, which is absent in the corresponding d-wave state in the U(1) theory. It has been pointed out that the existence of a mass gap in the U(1) theory may destabilize the d-wave state [16]. The sF phase may be more stable from this point of view. (2) The d-wave state in the U(1) theory does not produce the double-peak structure in the incoherent background of ImG. One needs to use a flux phase in the U(1) theory to produce the double peak (at the expense of breaking translation and time reversal symmetry [14]). (3) The d-wave state in the U(1) theory does not have Fermi pockets at finite doping, even if we include the gauge interaction as we did in the SU(2) theory. The SU(2) theory can generate Fermi pockets without breaking translation symmetry. Because of their nesting condition, the spin gap (sF) phase of the SU(2) theory can have a nonzero Pauli spin susceptibility (in $T \to 0$ limit) and strong antiferromagnetic spin fluctuations. Both properties have direct experimental consequences.

[1] See Z. X. Shen and D. S. Dessau, Phys. Rep. **253**, 1 (1995); Z. X. Shen *et al.*, Science **267**, 343 (1995).
[2] B. Shraiman and E. Siggia, Phys. Rev. Lett. **62**, 1564 (1989).
[3] See A. Millis and H. Monien, Phys. Rev. Lett. **70**, 2810 (1993); **71**, 210(E) (1993), for references.
[4] A. Kampf and J. R. Schrieffer, Phys. Rev. B **41**, 6399 (1990); **42**, 7967 (1990).
[5] P. W. Anderson, Science **235**, 1196 (1987).
[6] I. Affleck and J. B. Marston, Phys. Rev. B **37**, 3774 (1988).
[7] I. Affleck, Z. Zou, T. Hsu, and P. W. Anderson, Phys. Rev. B **38**, 745 (1988).
[8] G. Kotliar and J. Liu, Phys. Rev. B **38**, 5142 (1988); Y. Suzumura *et al.,* J. Phys. Soc. Jpn. **57**, 2768 (1988).
[9] H. Fukuyama, Prog. Theor. Phys. Suppl. **108**, 287 (1992).
[10] B. O. Wells *et al.*, Phys. Rev. Lett. **74**, 964 (1995).
[11] M. U. Ubbens and P. A. Lee, Phys. Rev. B **46**, 8434 (1992).
[12] X. G. Wen, Phys. Rev. B **44**, 2664 (1991).
[13] P. Beran, D. Poilblanc, and R. Laughlin, Report No. condmat/9505085.
[14] A chiral spin state also gives similar results; R. B. Laughlin, Phys. Rev. B **45**, 400 (1992).
[15] A. Moreo, S. Haas, A. Sandvik, and E. Dagotto, Phys. Rev. B **51**, 12 045 (1995).
[16] M. U. Ubbens and P. A. Lee, Phys. Rev. B **49**, 6853 (1994).